AVERAGE 120-KW MPC MODULATOR FOR PLASMA DE-NOX/DE-SOX SYSTEM*

J. S. Oh, S. D. Jang, Y. G. Son, M. H. Cho, W. Namkung, and D. J. Koh+
Pohang Accelerator Laboratory, POSTECH
San-31, Hyoja-dong, Pohang, 790-784, Republic of Korea

Abstract

The pulsed corona discharge process shows the encouraging results for the removal of NOx and SOx gases based on small-scale experiments. The lifetime and the reliability of the system are major difficulties to realize this newly developed technology because the downtime for maintenance affects the plant availability. The combination of a high power solid-state switch with a magnetic pulse compressor (MPC) is suitable scheme to meet these requirements. An average 120-kW MPC modulator has been constructed and tested with a plasma reactor for an industrial incinerator plant. The plasma reactor has wire-plate electrodes and can treat the gas of 50,000 Nm^3/Hr. This modulator can generate 150 kV pulses with 500 nsec (FWHM) pulse width, and 300 Hz repetition rate. This paper presents design details and the operational characteristics of the MPC modulator.

I. INTRODUCTION

Research activity on the plasma treatment of the flue gas that is toxic effluent gas such as SOx, NOx, and VOC's from the coal or oil burning power plants, has been extensively performed by many research institutes on small-scale experiments. In the experiments at the iron-ore sinter plant, we have demonstrated and evaluated the possibility of the pulsed corona process [1-3]. In order to supply necessary intense streamer corona to the flue gas, the high peak current and narrow high voltage pulse should be repetitively applied to the reactor. Therefore, issues on lifetime and reliability of the system are major difficulties for the practical large-scale industrial applications. Over 20 years of the research, there are few modest scale pilot plants for research purpose, whose gas flow rate well below 10,000 Nm^3/hr. The combination of a high power solid-state switch and saturable reactors as magnetic switches is suitable scheme to meet these requirements. Recently we have completed a pilot plant applied to an industrial waste incinerator with the incineration capacity of 30,000 ton/year. The plasma reactor is wire-plate type , and can treat the gas of 50,000 Nm^3/hr. An average 120-kW modulator has been constructed and applied to the reactor. This paper presents the initial test result and technical issues on the intense pulsed streamer discharge system for the simultaneous removal of SOx and NOx gases.

II. DESIGN OF MPC MODULATOR

The simplified circuit diagram of MPC modulator is shown in Fig. 1. This system utilizes two-stage magnetic pulse compressor that can generate 150 kV pulses with 500 nsec (FWHM) pulse width, and 300 Hz repetition rate. Table 1 summarizes the key design parameters of the MPC modulator.

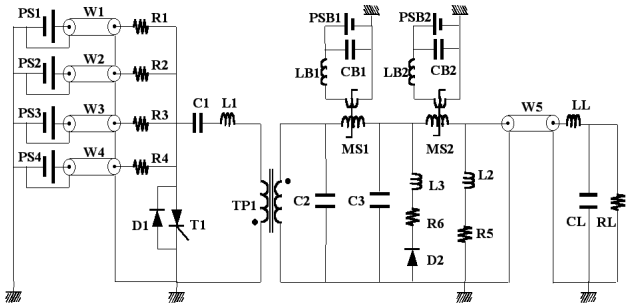

Figure 1. Circuit diagram of the MPC modulator.

Table 1. Design parameters of the MPC modulator.

Average power (kW)	120
Peak output voltage (kV)	150
Peak current (kA)	10
Pulse length (nsec, FWHM)	500
Pulse energy (J)	400-600
Pulse repetition rate (Hz)	300
Pulse efficiency (%)	70

The power supplies PS1 to PS4 (Dong-A High-Tech) are series-resonant inverters that charge a capacitor C1 up to 25 kV through protection resistors (from R1 to R4) and the primary winding of a pulse transformer TP1 (1 to 8 step-up ratio). The stored energy in C1 is transferred to C2 by a semiconductor switch T1. Then it is compressed by a first-stage magnetic switch MS1 and C3 . It is further compressed by a second-stage magnetic switch MS2 and transferred to a load. The corona reactor load is represented by a series inductance LL and a non-linear corona resistance RL in parallel with a varying capacitor CL [4]. The resistors R1 through R4 and freewheeling diode D1 protect the power supplies from inverse voltage. The reflected energy from the load due to the arcing is absorbed by R6. In order to keep the streamer corona from transforming to an arc, duration of the high voltage pulse must be restricted to less than 1-μsec, which is

* Work supported in part by Pohang Iron and Steel Company (POSCO), RIST, and MOST.
+ Air Protection Research Team, RIST, Republic of Korea

assisted by the resistor R5 with an inductor L2 [5]. The DC current sources PSB1, PSB2 reset the magnetic cores to provide matching flux swing. All resistors and a solid-state switch are installed in the independent panel and cooled by deionised water. Other high voltage components are immersed in transformer oil that is continuously circulated through an oil heat exchanger.

Reliable, long life and low maintenance switching of high peak current and di/dt capability for repetitive short pulses is now available technology [6]. The main switch T1 is a semiconductor switch assembly that is consisted of eight fast thyristors (ABB semiconductor AG; 5SPR-26L4508) stacked in series to generate high power pulses (12.6 kA, 7 μsec) at 20 kV and 300 pulses per seconds. Each switch element is a reverse conducting pulsed power device with blocking voltage of 4.5 kV. The element has 91 mm diameter silicon wafer as an active part, and the freewheeling diode is built in the same silicon wafer. The gate driver unit is integrated with the semiconductor switch element to minimize the line inductance in providing the current pulse to the gate as shown in Fig. 2.

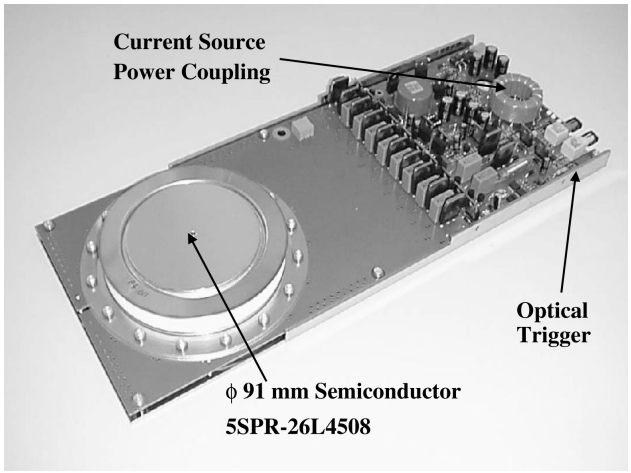

Figure 2. Integrated solid-state switch 5SPR-26L4508.

Table 2. The design parameters of two magnetic switches.

Maximum core flux density swing (T)	3.4
Core sectional area (cm^2)	152
Coil sectional area (cm^2)	366
Mean flux path length (cm)	94
Peak voltage (kV)	200

Two-stage MPC circuit is designed according to the principle of I. Druckmann [7]. Design parameters of the two magnetic switches are listed in table 2. The magnetic switch has three toroidal sub-cores in parallel on the Teflon mandrel, which is made of 2605CO Metglass amorphous metals (15 μm thick, 2" wide sheet). The core mass of a switch is about 70 kg. Total core loss is estimated to be about 6-kW at the full power operation. Therefore, magnetic switches are cooled by forced oil convection.

III. PERFORMANCE OF MPC MODULATOR

The typical voltages measured by capacitive voltage dividers at the capacitor C2 (CVD1), C3 (CVD2) and output terminal (CVD3) are shown in Fig. 3. The capacitor C1 is charged to 18.2 kV by the high voltage inverter power supply. While the energy is transferred from C1 to C2, the first magnetic switch MS1 holds off the current by presenting a large inductance to the circuit. It then saturates allowing the energy to flow to C3. After the saturation of the second magnetic switch MS2, the energy flows to the reactor load. The peak voltage is 120 kV at the reactor load.

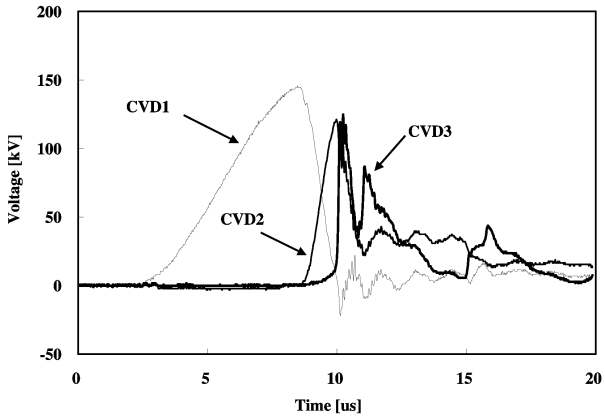

Figure 3. Voltage waveforms.

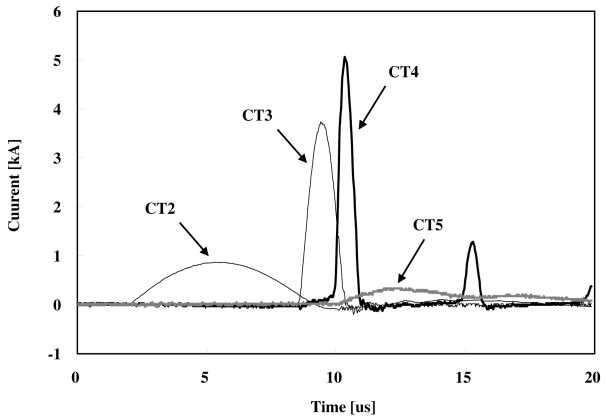

Figure 4. Current waveforms.

Figure 4 shows the corresponding current waveforms, transformer secondary current (CT2), MS1 switch current (CT3), MS2 switch current (CT4), tail resistor current (CT5). The net reactor current is the deference between CT4 current and CT5 current. The peak current is 5-kA and the pulse width (FWHM) is about 500 ns at the reactor load.

The energy efficiency is the ratio of the pulse energy transferred to the reactor and the initial energy charged on the first capacitor C1. The pulse energy transferred to the plasma reactor and the energy dissipated at the resistor R5 are calculated by integrating the product of the voltage and current waveforms as shown in Fig. 5. The energy

delivered to the reactor is 214 J and the absorbed energy at the resistor R5 is 53 J. It is clearly seen that the pulse energy remaining in the reactor capacitance is absorbed by the resistor R5. The energy stored in C1 is 332 J at 18.2 kV. Therefore, the energy efficiency of the MPC modulator is 64%. The loss at the parallel resistor R5 is 16%. The high voltage inverter power supply has internal loss in power conversion, which results 90% charging efficiency. Considering these losses, the overall energy efficiency from the wall plug to the reactor load is about 60%.

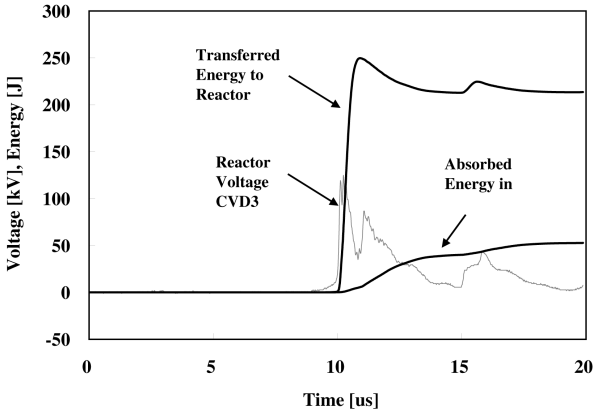

Figure 5. Transferred energy to the reactor and absorbed energy in the resistor R5

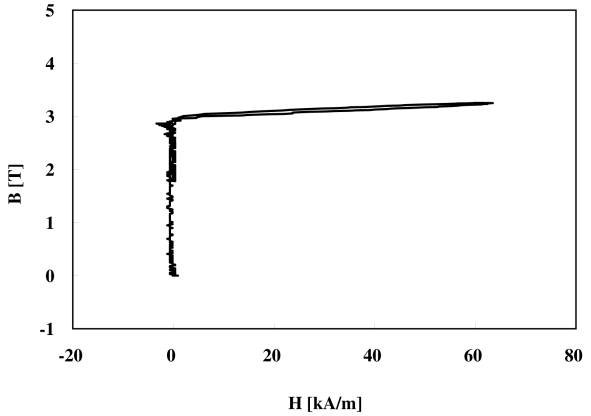

Figure 6. B-H curve of the magnetic core of MS1.

Figure 6 is the analysed B-H curve of the magnetic core of the MS1 switch by using voltage and current waveforms. It shows that the high relative permeability of the core is drastically dropped to 3.3 after the core is driven to saturation over 3 T. The peak coercive field strengths are fairly larger than 10 kA/m so that they are enough to guarantee the full saturation of cores.

IV. DE-NOX/DE-SOX APPLICATION

Positive high voltage pulse applied to the discharging electrode induces streamer corona discharges, rapidly growing toward the grounded plate. Free electrons gain energy from an imposed electric field, and during their drift, they lose energy through collisions with neutral gas molecules such as O_2, N_2 and H_2O. Chemically active species such as O, OH, HO_2 and O_3 can be formed from the electron-molecule collisions, and they can convert SOx and NOx into sulphuric acid and nitric acid [8]. The sulphuric acid and nitric acid can be neutralized by ammonia usually used in pulse corona discharge process. In such a case, ammonium sulphate and ammonium nitrate are obtained as the final products of SOx and NOx removal.

Figure 7 depicts the schematic of the pilot plant for pulsed corona processing system installed at an industrial incinerator. The processing chamber is composed of two series reactors. The first one is the pulsed corona reactor (PCR) to remove SOx and NOx using a magnetic pulse compressor (MPC), and the second one is the electrostatic precipitator (ESP) to collect the by-products such as ammonium sulphate and ammonium nitrate using a micro-pulse system (MPS).

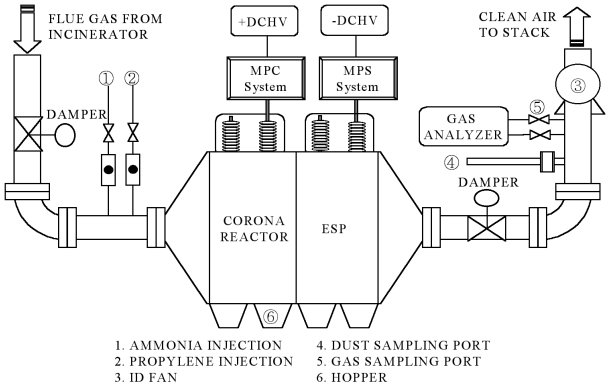

Figure 7. Schematic of the pilot plant for pulsed corona discharge processing system.

Table 3. Main parameters of pulsed corona reactor.

Gas flow rate (Nm^3/hr)	50,000
Gas temperature (^oC)	160-190
GP (Gas Passage) number	10
GP size, W x H x L (m)	3.0 x 4.1 x 4.0
Total wire length (m)	480
Wire diameter (mm)	10
Distance between plates (mm)	300

Main parameters of the corona reactor are shown in table 3. The reactor structure is almost identical to a typical electrostatic precipitator. The PCR has ten gas passages (GP). Each GP is 30-cm wide, 4.1-m high and 4.0-m long. It has 12 discharge wires with effective length of 4 m and the diameter of 10-mm. The geometric capacitance of this reactor is approximately 10 nF.

Figure 8 shows the SOx and NOx removal characteristics. The gas flow rate of the flue gas is 42,000 Nm^3/h at the temperature of 170^{o}C. The specific energy P/Q defined as the ratio of input power P [W] to gas flow rate Q [Nm^3/hr] is approximately 1.4 Wh/Nm^3 based on discharging power. To improve removal efficiency of the concentration of SOx and NOx, ammonia (NH_3) and propylene (C_3H_6) are used as chemical additives. The role of propylene in NOx removal is well described in our

previous study [1-3]. The concentrations of NH_3 and propylene used as additives were 370 ppm and 55 ppm, respectively. In this experimental condition, inlet SOx concentration of 100-120 ppm decreased to nearly 0 ppm, which is equivalent to SOx removal efficiency of about 99%. Inlet NOx concentration of 70-75 ppm is decreased to 20ppm, which corresponds to NOx removal efficiency of 70%.

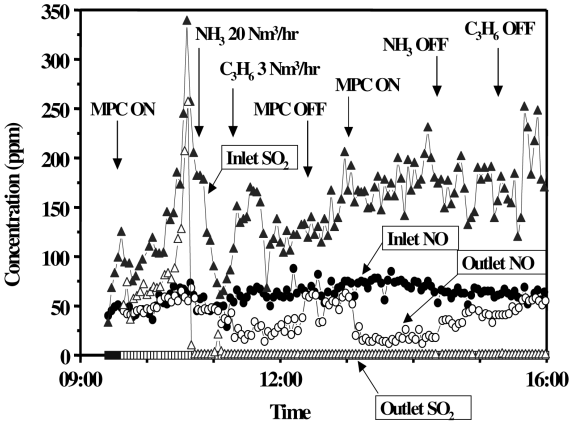

Figure 8. SOx and NOx removal characteristics.

V. SUMMARY

The 120-kW MPC modulator has been developed and its performance is tested with a corona process reactor that can treat the flue gas of 50,000 Nm^3/hr of an industrial incinerator for the removal of SOx and NOx. We employed a semiconductor switch stack assembly and two-stage magnetic pulse compressors. The typical energy transfer efficiency is 64% when the corona reactor is operated at 120kV. The SOx removal efficiency of 99% is easily achievable with NH_3 addition. The NO removal efficiency is 70% with the inlet concentration of 75 ppm using C_3H_6 addition under specific energy input of 1.4 Wh/Nm^3. Proper amount of C_3H_6 additive is critical to increase NO removal efficiency but the additive concentration should be limited to avoid the slippage. In the further experiment, we plan to demonstrate the reliability of main HV components and MPC system suitable for the industrial application of the pulse corona processing. The improvement of energy efficiency is also expected through the understanding of the corona phenomena to process parameters such as concentrations of O_2, SOx, NOx, dust, and flue gas temperature and humidity, etc.

VI. REFERENCES

[1] Y. S. Mok, S. W. Ham, and I. Nam, “Evaluation of energy utilization efficiencies for SO2 and NO removal by pulsed corona discharge process,” Plasma Chem. Plasma Proc., vol. 18, no. 4, pp. 535-550, 1998.

[2] Y. S. Mok, I. Nam, R. W. Chang, S. W. Ham, C. H. Kim, and Y. M. Jo, “Application of positive pulsed corona discharge to removal of SO2 and NOx,” in Proc. 7th Int. Conf. Electrostatic Precipitation, Hilton, Kyungju, Korea, 1998, pp. 270-277

[3] Y. S. Mok, I. S. Nam, “Positive Pulsed Corona Discharge for Simultaneous Removal of SO2 and NOx from Iron-Ore Sintering Flue Gas,” IEEE Trans. on Plasma Science, Vol. 27, No. 4, pp. 1188-1996, August 1999.

[4] G. Dinelli, L. Civitano, and M. Rea, “Industrial experiments on pulse corona simultaneous removal of NOx and SO2 from flue gas,” IEEE Trans. Ind. Application, vol. 26, pp. 535-541, May/June 1990.

[5] J. J. Lowke and R. Morrow, “Theoretical analysis of removal of oxides of sulphur and nitrogen in pulsed operation of electrostatic precipitators,” IEEE Trans. Plasma Sci., vol. 23, pp. 661-671, Aug. 1995.

[6] A. Welleman, U. Schapbach, E. Ramezani, “Plug and Play Solid State Switching System for Laser Application,” 12th IEEE Pulsed Power Conf., Monterey, CA, pp. 150-152, 1999

[7] Druckmann, S. Gabay and I. Similanski, “A new Algorithm for the Design of Magnetic Pulse Compressors,” Conf. Record of the 1992 Twentieth Power Modulator Symposium, Myrtle Beach, SC, pp. 213-216, 1992

[8] Ivo Gallimberti, "Impulse Corona Simulation for Flue Gas Treatment," Pure & Appl. Chem., Vol. 60, No. 5, pp. 663-674, 1988